

Dielectric Properties of Ice and Liquid Water from First-Principles Calculations

Deyu Lu,^{1,*} François Gygi,² and Giulia Galli¹

¹*Department of Chemistry, University of California, Davis, Davis, California 95616, USA*

²*Department of Applied Science, University of California, Davis, Davis, California 95616, USA*

(Received 16 October 2007; published 8 April 2008)

We present a first-principles study of the static dielectric properties of ice and liquid water. The eigenmodes of the dielectric matrix ϵ are analyzed in terms of maximally localized dielectric functions similar, in their definition, to maximally localized Wannier orbitals obtained from Bloch eigenstates of the electronic Hamiltonian. We show that the lowest eigenmodes of ϵ^{-1} are localized in real space and can be separated into groups related to the screening of lone pairs, intra-, and intermolecular bonds, respectively. The local properties of the dielectric matrix can be conveniently exploited to build approximate dielectric matrices for efficient, yet accurate calculations of quasiparticle energies.

DOI: [10.1103/PhysRevLett.100.147601](https://doi.org/10.1103/PhysRevLett.100.147601)

PACS numbers: 77.22.-d, 71.15.-m, 71.45.Gm, 78.20.Ci

The physical and chemical properties of water are of fundamental importance in numerous fields of science, including planetary physics, chemistry, and biology [1]. Experimental techniques such as x-ray and neutron diffraction [2] have provided structural information on both ice and liquid water, and their electronic and optical properties have been probed by x-ray Raman and x-ray absorption spectroscopy [3]. Nevertheless, many open questions remain on the ionic, electronic and bonding structure of water, including the interpretation of recent spectroscopic data [4]. From a theoretical point of view, *ab initio* calculations based on density functional theory (DFT) [5] have been shown to qualitatively account for various structural and dynamical properties of ice and water [6,7]. However, excited state properties may not be evaluated satisfactorily using the standard local density approximation (LDA) or generalized gradient approximation (GGA) to DFT, pointing at the importance of exchange-correlation effects [8] in the calculation of electronic and optical spectra, as discussed in two recent studies of ice [9] and water [10] based on many-body perturbation theory (MBPT).

One key input in MBPT (and in time-dependent DFT calculations) is the dielectric matrix $\epsilon(\mathbf{r}, \mathbf{r}'; \omega)$. In spite of its central role in excited states calculations and hence, in the interpretation of spectroscopic data, very little is known about the screening properties of ice and water at the microscopic scale.

In this Letter, we present a first-principles study of the static dielectric properties of ice and liquid water, and discuss locality properties of their respective dielectric matrices, in particular, those of the lowest eigenmodes of ϵ^{-1} , which are essential to the concept of intra- and intermolecular screening. We also propose an approximate way to represent the full dielectric matrix that enables efficient calculations of quasiparticle energies within the *GW* approximation [11].

In this study liquid water was modeled by a periodic system containing 16 H₂O molecules in a cubic unit cell with size of 14.80 a.u.. A recent investigation [10] with a

similar unit cell size yielded both quasiparticle band gap and optical spectra in satisfactory agreement with experiment. Atomic positions were obtained through classical molecular dynamics simulations [12] with the TIP4P potential [13]. The electronic wave functions were computed within DFT-PBE [14] using a plane-wave basis set with a kinetic energy cutoff of 60 Ry, and separable, norm-conserving pseudopotentials [15,16]; the Brillouin zone (BZ) was sampled with 64 *k* points (a 4 × 4 × 4 Monkhorst-Pack grid). Both band structure and density of states (not shown) are found to be in good agreement with previous DFT calculations with larger unit cells [17]. Calculations on hexagonal ice (ice *Ih*) were based on the Bernal ice model [18], where the optimized cell parameters are *a* = 14.53 a.u. and *c* = 13.67 a.u.. For ice we employed a kinetic energy cutoff of 85 Ry and 64 *k* points for BZ sampling. Quasiparticle calculations were carried out within the *G*₀*W*₀ approximation [11,19–21], where the frequency dependence of the self-energy was approximated by a plasmon-pole model [22] based on dielectric eigenmodes (DMs).

In the following, we first discuss the properties of the static dielectric matrices of ice and water, as obtained within the random phase approximation (RPA) [23]. In particular we compare eigenvalues and eigenvectors of these matrices with those obtained with a similar procedure for the gas phase water monomer and dimer. Finally, by exploiting localization properties found for the eigenvectors of ϵ^{-1} , we propose a way of constructing approximate, yet accurate dielectric matrices for electronic structure calculations with MBPT.

The macroscopic dielectric constants can be extracted from the inverse dielectric matrices $\epsilon_{\mathbf{GG}'}^{-1}(\mathbf{q})$ as $\epsilon_M = 1/\epsilon_{0,0}^{-1}(0)$. Our calculations yield $\epsilon_M^{\text{ice}} = 1.78$ and $\epsilon_M^{\text{water}} = 1.72$, in satisfactory agreement with the experimental value of about 1.7 and 1.8 [24]. The dielectric band structures (DBS's) [25], shown in Figs. 1(a) and 1(b), overall exhibit very little dispersion suggesting, in analogy with flat electronic band structures, a strong localization of the eigen-

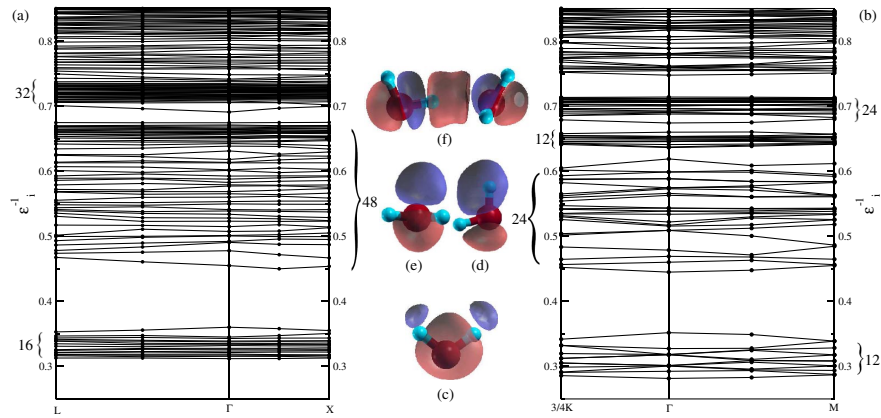


FIG. 1 (color online). The dielectric band structure of (a) liquid water and (b) ice *Ih*. The lowest bands in ice and water form distinctive groups, whose representative maximally localized dielectric eigenmodes (see text) are shown in (c),(d),(e), and (f).

states of ϵ^{-1} with respect to the unit cell size. We note that the lowest eigenvalue at the Γ point in ice (water) is 0.28 (0.31), corresponding to a dielectric screening constant of 3.55 (3.21) much larger than ϵ_M^{ice} ($\epsilon_M^{\text{water}}$). From the lowest part of the ice spectrum ($\epsilon_i^{-1} < 0.75$ in Fig. 1(a) with ϵ_i^{-1} the i th eigenvalue of ϵ^{-1}), one can identify four groups of eigenvalues, each containing a number of bands that is a multiple of the number of molecules (n_m) in the unit cell: the four groups, in order of increasing eigenvalues, contain n_m , $2n_m$, n_m and $2n_m$ bands, respectively. Very similar features were identified in the DBS of water except for the mixing of eigenvalues belonging to group two and three. Furthermore, group one and four in average have larger eigenvalues in water than in ice, possibly due to a higher level of structural disorder in the liquid phase.

The eigenfunctions of ϵ^{-1} represent potentials which, when applied to the system, yield a screened potential of the same spatial form, but reduced by a factor given by the inverse of the eigenvalue. In a periodic system, these eigenfunctions are Bloch waves extending over the entire unit cell in real space. In order to extract screening properties at the atomic scale, and relate them to specific bonds, we explored the possibility of transforming extended eigenfunctions at the Γ point into localized states. To this end, within the distinct groups of eigenvectors identified above, we applied the same procedure proposed in Ref. [26] that transforms extended Bloch states of the Hamiltonian into maximally localized Wannier functions [27], following a simultaneous diagonalization algorithm [28]. We shall refer to this representation of dielectric eigenmodes as maximally localized dielectric eigenmodes (MLDMs). Those MLDMs obtained from the first three groups can be associated to intramolecular screening. In the first group, the majority of the MLDMs is centered around the oxygen atom with a smaller intensity in proximity of the hydrogen atoms, as shown in Fig. 1(c). The MLDMs originating from modes of the second and third groups are associated with intramolecular O-H bonds [Fig. 1(d)] and oxygen lone pair p like functions [Fig. 1(e)], respectively. The spatial extension of

MLDMs increases in going from group one to group three, and the average spreads of MLDMs in ice are 1.04, 2.22, and 2.75 a.u., respectively.

Dielectric bands in the fourth group have an intermolecular character. In ice, MLDMs from group four represent the screening within nearest neighbors (water pairs) as shown in Fig. 1(f): the function has a significant amplitude both along the O-H bond of the donor and on the oxygen atom of the acceptor. The Wannier center is located in proximity of the donor proton, and the weight of the MLDM associated with the donor is larger than that on the acceptor. This results in a relatively small average spread of 2.19 a.u.. The corresponding mode in liquid water is less localized in real space, with an average spread of 2.69 a.u.. MLDMs beyond the fourth group in both systems become strongly entangled and more delocalized, and cannot be ascribed to specific intra- or intermolecular bonds.

The nature of MLDMs of water in solid and liquid phases can be elucidated by comparisons with the DMs of an isolated water monomer and dimer [29], as obtained

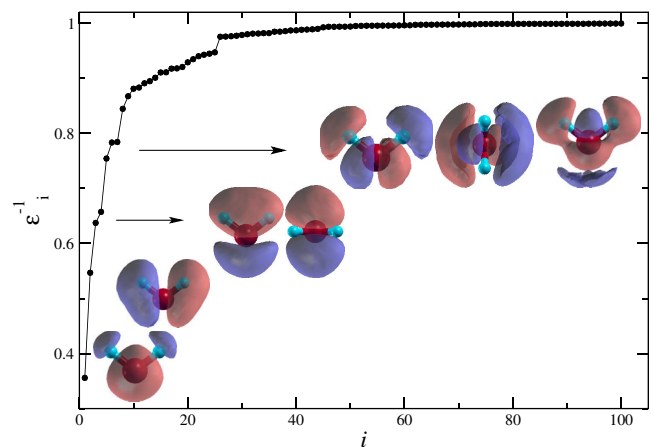


FIG. 2 (color online). The eigenvalues and first seven eigenfunctions of the inverse dielectric matrix of an isolated water molecule.

by direct diagonalization of their RPA dielectric matrices. As shown in Figs. 1 and 2, the intramolecular modes of liquid water and ice can be traced back to those of an isolated monomer; in particular, the modes associated with the bulk O-H bond [two per molecule as shown in Fig. 1(d)] are a linear combination of the second and third DMs of the monomer. For the same type of modes, the eigenvalues in the monomer are always larger than the average of those of the bulk. Furthermore, there is no eigenmode present in the monomer at $0.66 < \epsilon_i^{-1} < 0.75$, i.e., the range of eigenvalues corresponding to the pair screening modes in the bulk. These modes can instead be traced back to those found in a water dimer (not shown), although the corresponding eigenvalue is higher ($\epsilon_i^{-1} \approx 0.77$) than in the bulk. This difference may be ascribed to the different geometry of hydrogen bonds in the dimer and the bulk, and to the presence of the local field created by the dielectric environment present in the bulk tetrahedral network. These findings indicate that a description of liquid water as a collection of molecules with modified polarizabilities, with respect to their gas phase values, would not be appropriate, as it would not capture important properties of the system dielectric response, which includes complex intermolecular screening.

In order to quantify the contribution of localized modes to the overall dielectric screening, we plot $(1 - \epsilon_i^{-1})$ in Fig. 3. Clearly the curve decays very rapidly as the mode index i increases. The intramolecular and nearest-neighbor modes alone contribute nearly 50% of the screening as shown in the inset. This suggests a way to reconstruct an approximate dielectric matrix from a limited number of DMs. We write ϵ^{-1} as the sum of two terms,

$$\epsilon^{-1} \simeq \sum_{i=1}^n |U_i\rangle \epsilon_i^{-1} \langle U_i| + \sum_{i=n+1}^N |V_i\rangle \epsilon_{Ai}^{-1} \langle V_i|. \quad (1)$$

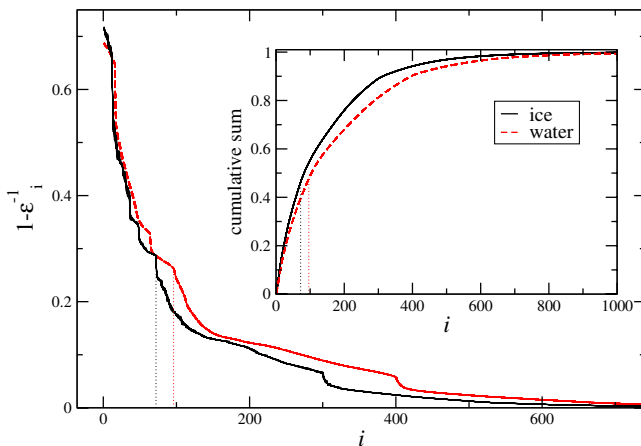


FIG. 3 (color online). Dielectric screening characterized by $(1 - \epsilon_i^{-1})$ in water (dashed line) and ice (solid line), as a function of the dielectric eigenmode index. The normalized cumulative sum in the inset shows that nearly 50% of the screening arises from intramolecular and nearest-neighbor modes (lying to left of the dotted lines).

The first term contains the lowest n exact DMs, and the second term contains approximate forms of eigenvalues ϵ_{Ai}^{-1} and eigenvectors $|V_i\rangle$ for $i > n$, as described below. Eigenvectors $|U_i\rangle$ and $|V_i\rangle$ are required to be orthogonal, although this requirement is not sufficient to uniquely determine $|V_i\rangle$. Within a Fourier representation and plane-wave basis sets, the initial guesses for $|V_i\rangle$ were chosen as plane waves, and orthogonalization was enforced by a Gram-Schmidt procedure. We adopted the Penn dielectric function [30] for $\epsilon_{Ai}^{-1}(\mathbf{q})$,

$$\epsilon_{Ai}^{-1}(\mathbf{q}) = \left\{ 1 + \left(\frac{E_p}{E_g} \right)^2 F \left[1 + \frac{p_i^2(\mathbf{q})}{(\hbar k_F)^2} \frac{E_F}{E_g} F^{1/2} \right]^{-2} \right\}^{-1}, \quad (2)$$

where $F = 1 - \frac{1}{4}(E_g/E_F)$ and $p_i^2(\mathbf{q}) = \langle V_i(\mathbf{q}) | \mathbf{p}^2 | V_i(\mathbf{q}) \rangle$ with \mathbf{p} the momentum operator; E_p , E_F , and k_F are plasmon energy, Fermi energy, and Fermi wave vector, respectively. Once E_g is determined from $\epsilon_1^{-1}(0)$, there is no free parameter in this model. To test the validity of our approximation in describing excited state properties, we computed quasiparticle band gaps, the energy difference between the highest occupied molecular orbital (HOMO) and the lowest unoccupied molecular orbital (LUMO) at the Γ point, by using the full and approximate dielectric matrices. With the full dielectric matrix we obtained a quasiparticle band gap of 8.7 eV for water, in agreement with other theoretical (8.6 eV) [10] and experimental (8.7 ± 0.5 eV) [31] studies. A simple truncation of the second term in Eq. (1) results in a slow convergence of quasiparticle band gaps as shown in Fig. 4. The band gap is overestimated when n , the number of exact modes included in Eq. (1), is insufficient, due to an underestimate of the screening. Compared to the truncation scheme, the band gap obtained by using both terms in

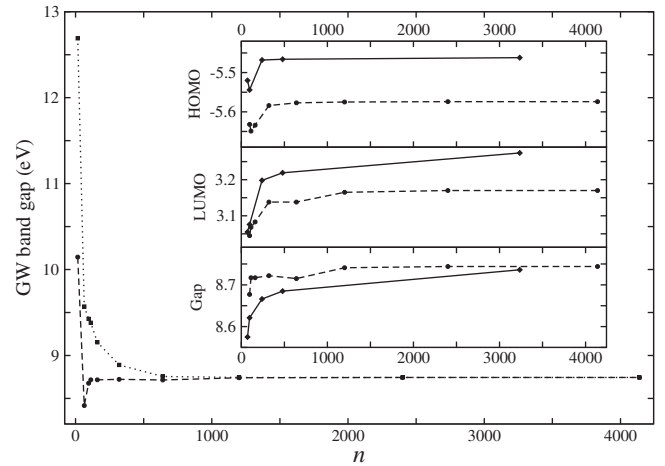


FIG. 4. Dependence of quasiparticle (GW) band gap of liquid water on the number of exact dielectric eigenmodes (n) used in Eq. (1). Dotted line: only the first term on the right hand side of Eq. (1) is included (truncated ϵ^{-1}); dashed line: both terms are included (approximate ϵ^{-1}). Inset: Convergence of quasiparticle energies (HOMO and LUMO) and band gap of ice (solid line) and water (dashed line) as a function of n when an approximate dielectric matrix is used.

Eq. (1) requires a much smaller n , e.g., 96 instead of about 600 in the case of water. By including up to the nearest-neighbor screening modes, the band gap is already within 0.07 (0.16) eV of the results obtained from the full dielectric matrix for water (ice). About the same number of eigenmodes is required to converge the absolute value of the HOMO and LUMO energies (see inset). We note that the procedure proposed here can lead to substantial savings in memory and computer time, when computing quasiparticle spectra. Indeed, the lowest n DMs can be obtained through iterative approaches [32,33], thus avoiding the evaluation and diagonalization of the full dielectric matrix, as well as the expensive direct summation over the unoccupied states in the dielectric response function calculation.

In conclusion, we presented a microscopic description of the static, electronic dielectric response of liquid water and ice from first-principles. We identified dielectric eigenmodes that can be localized in real space, and that are related to intra- and intermolecular screening within nearest-neighbors. We also proposed an approximate yet accurate way to construct the static dielectric matrix, that may be exploited to efficiently obtain quasiparticle spectra. Our approach opens the way to the study of excited state properties of large water samples and possibly solvated molecules using MBPT.

This work was supported by DOE SciDAC Grant No. DE-FC02-06ER25794, and the computational resource was provided by San Diego Supercomputer Center under grant No. DMR060039N and DMR060034T. Discussions with Lucia Reining, Manu Sharma, Davide Donadio, Yan Li, and Hugh Wilson are gratefully acknowledged.

*dylu@ucdavis.edu

- [1] See, e.g., F. Franks, *Water: A Matrix of Life* (Roy. Soc. Chem., Cambridge, United Kingdom, 2000), 2nd ed.
- [2] T. Head-Gordon and M. E. Johnson, Proc. Natl. Acad. Sci. U.S.A. **103**, 7973 (2006); A. K. Soper, J. Phys. Condens. Matter **19**, 335206 (2007), and references therein.
- [3] M. Leetmaa *et al.*, J. Chem. Phys. **125**, 244510 (2006), and references therein.
- [4] Ph. Wernet *et al.*, Science **304**, 995 (2004); J. D. Smith *et al.*, Science **306**, 851 (2004).
- [5] P. Hohenberg and W. Kohn, Phys. Rev. **136**, B864 (1964); W. Kohn and L. J. Sham, Phys. Rev. **140**, A1133 (1965).
- [6] J. C. Grossman, E. Schwegler, and G. Galli, J. Phys. Chem. B **108**, 15865 (2004); E. Schwegler, J. C. Grossman, F. Gygi, and G. Galli, J. Chem. Phys. **121**, 5400 (2004).
- [7] J. VandeVondele *et al.*, J. Chem. Phys. **122**, 014515 (2005), and references therein.
- [8] M. Rohlfing and S. G. Louie, Phys. Rev. B **62**, 4927 (2000); G. Onida, L. Reining, and A. Rubio, Rev. Mod. Phys. **74**, 601 (2002).
- [9] P. H. Hahn *et al.*, Phys. Rev. Lett. **94**, 037404 (2005).
- [10] V. Garbuio, M. Cascella, L. Reining, R. Del Sole, and O. Pulci, Phys. Rev. Lett. **97**, 137402 (2006).
- [11] L. Hedin, Phys. Rev. **139**, A796 (1965).
- [12] http://www.cse.scitech.ac.uk/ccg/software/DL_POLY/.
- [13] W. L. Jorgensen *et al.*, J. Chem. Phys. **79**, 926 (1983).
- [14] J. P. Perdew, K. Burke, and M. Ernzerhof, Phys. Rev. Lett. **77**, 3865 (1996).
- [15] L. Kleinman and D. M. Bylander, Phys. Rev. Lett. **48**, 1425 (1982).
- [16] N. Troullier and J. L. Martins, Phys. Rev. B **43**, 1993 (1991).
- [17] D. Prendergast, J. C. Grossman, and G. Galli, J. Chem. Phys. **123**, 014501 (2005).
- [18] J. D. Bernal and R. H. Fowler, J. Chem. Phys. **1**, 515 (1933).
- [19] M. S. Hybertsen and S. G. Louie, Phys. Rev. Lett. **55**, 1418 (1985).
- [20] In the dielectric response calculation of liquid water (ice), we employed a cutoff of 33.70 (40.03) Ry to represent the wave functions and a cutoff of 17.84 (18.08) Ry for the size of the dielectric matrix, and included 436 (400) empty bands. A total number of 624 (608) bands were included in the self-energy calculation, and 13 805 (10 737) plane waves (39.82 and 40.03 Ry) were used to evaluate the exact exchange part of the self-energy.
- [21] X. Gonze *et al.*, Comput. Mater. Sci. **25**, 478 (2002); X. Gonze *et al.*, Z. Kristallogr. **220**, 558 (2005); The ABINIT code is a common project of the Université Catholique de Louvain, Corning Incorporated, and other contributors (URL <http://www.abinit.org>).
- [22] W. von der Linden and P. Horsch, Phys. Rev. B **37**, 8351 (1988).
- [23] S. L. Adler, Phys. Rev. **126**, 413 (1962); N. Wiser, Phys. Rev. **129**, 62 (1963).
- [24] G. P. Johari and S. J. Jones, Proc. R. Soc. A **349**, 467 (1976); B. Bagchi, Chem. Rev. **105**, 3197 (2005).
- [25] A. Baldereschi and E. Tosatti, Solid State Commun. **29**, 131 (1979).
- [26] F. Gygi, J.-L. Fattebert, and E. Schwegler, Comput. Phys. Commun. **155**, 1 (2003).
- [27] N. Marzari and D. Vanderbilt, Phys. Rev. B **56**, 12847 (1997).
- [28] http://eslab.ucdavis.edu/software/Qbox/qbox_home.htm.
- [29] For both monomer and dimer calculations, we used a fcc supercell of $a = 35.36$ a.u. and an energy cutoff of 60 Ry; 985 bands were included to compute the dielectric matrix and the spurious interaction between image cells was removed according to the procedure suggested in G. Onida, L. Reining, R. W. Godby, R. Del Sole, and W. Andreoni, Phys. Rev. Lett. **75**, 818 (1995).
- [30] D. R. Penn, Phys. Rev. **128**, 2093 (1962).
- [31] A. Bernas, C. Ferradini, and J.-P. Jay-Gerin, Chem. Phys. **222**, 151 (1997).
- [32] S. Baroni, P. Giannozzi, and A. Testa, Phys. Rev. Lett. **58**, 1861 (1987).
- [33] H. Wilson, F. Gygi, and G. Galli (unpublished).